



Original article

Effects of plasma electrolytic polishing on SLM printed microfluidic platform

***Izidor Sabotin^a, Marko Jerman^a, Andrej Lebar^a, Joško Valentinčič^a,
Toni Böttger^b, Lisa Kühnel^b, Henning Zeidler^b**

^a University of Ljubljana, Faculty of Mechanical Engineering, Chair of Manufacturing Technologies and Systems, Aškerčeva ulica 6, 1000 Ljubljana, Slovenia

^b Technical University Bergakademie Freiberg, IMKF, Chair of Additive Manufacturing, Agricolastrasse 1, 09599 Freiberg, Germany

ABSTRACT

Additive manufacturing (AM) of metallic parts is gaining momentum in production industries. In view of producing a metal microproduct using AM the issue of high surface roughness is prominent. Plasma electrolytic Polishing (PeP) is a post processing technology that greatly reduces surface roughness of metallic parts. In this paper the effects of PeP of microfluidic platform, printed with selective laser melting (SLM) technology, is presented. The results show that surface roughness of the specimens was severely reduced. Also, some geometrical defects inherent to SLM technology were partly removed. It is shown, that for smaller geometrical microfeatures (sizes of less than 0.5 mm) the effectiveness of PeP is reduced. Through this investigation it can be concluded that PeP is a promising post-processing technology for SLM printed microparts since it significantly improves the overall part quality. However, further improvements of the process chain need to be implemented in order to render the microfluidic platform functional.

Key words: Selective laser melting, Plasma electrolytic polishing, Microfluidics, Additive manufacturing;

1. INTRODUCTION

In the past two decades Additive Manufacturing (AM), popularly denoted as 3D printing, gained significant interest and has been spoken of as a disruptive technology. With AM technology predominantly polymer based materials as well as metallic materials can be manufactured. In AM a part is built stepwise in a layer by layer fashion. Since in the process of building the part the material is added, it opens up the possibility to complex part designs which cannot be manufactured by subtractive processes. AM also enables short lead-times at relatively low costs. Nowadays, AM has been successfully utilized in many areas such as aerospace, automotive, electronics, medical and biomedical industries where highly specialized and customizable parts are required [1,2]. Microfluidics is a research field that greatly embraced the AM technologies. The attraction stems from two aspects of AM technologies [1]. The first aspect relates to the ability

to produce truly three-dimensional features. The second aspect relates to the ability to rapidly realize a 3D microfluidic device from constructed 3D model. This enables researchers to adopt the strategy of “fail fast and often”. Presently used AM technologies in microfluidics are inkjet 3D printing, fused deposition modelling, stereolithography and two photon polymerisation. Enlisted technologies are predominantly polymer based. On the other hand the utilization of metallic materials in microproducts has gained momentum, largely due to its superior properties in view of microproduct performance [3]. Steel microfluidic platforms have several benefits over polymer based such as high robustness, being operational under elevated temperatures and pressures, compatibility with organic solvents and yielding high thermal conductivity coefficients [4]. Among the AM technologies that can print metallic parts direct energy deposition (DED), selective laser sintering (SLS) and selective laser melting (SLM) are the most

* Corresponding author's.e-mail: izidor.sabotin@fs.uni-lj.si

Published by the University of Novi Sad, Faculty of Technical Sciences, Novi Sad, Serbia.
This is an open access article distributed under the CC BY-NC-ND 4.0 terms and conditions

promising to be utilized in future microfluidic applications [5]. In the view of their implementation SLM has some advantages compared to the former two. SLM exhibits better resolution than DED and it does not need additional processing step, namely sintering, as it is the case with SLS. SLM is a powder-bed fusion process. A layer of powder is first spread on the build substrate. In the next step laser beam scans the area related to the particular slice of the part geometry. The exerted heat melts the powder which after solidification joins with the adjacent regions and forms a solid metallic layer. In the next step a new layer of powder is applied to the part surface by a powder-recoating system and the lasers scans the region of the next part geometry slice. The process is repeated until the whole part is built. An inherent disadvantage of SLM as well as for all metallic AM technologies is the achievable surface quality. Namely, partial melting and/or agglomeration of powder on the surrounding regions of the melt pool leads to high roughness in the range of 10 μm to 30 μm of Ra [6]. For many applications, and especially in microfluidics, these values are inadequate, thus surface finishing is required. A promising surface finish technology is plasma electrolytic polishing (PeP) [7].

PeP has gained attention in the metal finishing industry due to its capability to considerably enhance surface properties [8]. PeP is an innovative surface treatment, which renders smooth, high-gloss surfaces with improved corrosion resistance. The process is primarily determined by the dissolution of the anode (the workpiece) and plasma-chemical reactions. Commonly, the part to be polished is immersed in the electrolyte bath and DC current is applied between the anode/part and cathode. Advantageous aspects of PeP stem from being able to process complex 3D-shaped parts simultaneously over its entire surface and the use of environmentally friendly aqueous electrolytes. The processing temperature at the part surface does not exceed the electrolyte boiling temperature which is below 120 °C. In this paper a process chain for microfluidic platform consisting of SLM printing and PeP post processing is evaluated through dimensional characterization. Geometrical features of the planar microfluidic platform consist of microchannels and microgrooves, embedded on the microchannel floor, which are commonly applied in bottom groove micromixers.

2. MATERIALS AND METHODS

2.1. SLM 3D printer

For 3D printing of sample microfluidic platforms EOS M 290 SLM printer based on powder-bed fusion was used. It utilises Yb-fibre laser with maximum beam power of 400 W and a laser focus point of 100 μm . Materialise Magics Metal Package and EOSPRINT software was used for CAD/CAM settings.

2.2. SLM printing process parameters

Default process parameters suggested by the CAD/CAM software considering the material and layer depth were

applied: laser beam power of 285 W, scanning speed of 960 mm/s, line ‘stripes’ scanning strategy, hatch spacing of 0.11 mm, powder layer depth of 0.04 mm, N₂ working atmosphere (cca. 0.15% O₂) and the thickness of support layers of 5 mm. EOS Maraging Steel MS1 powder material was used (X3NiCoMoTi 18-9-5) with a predicted relative density of parts of 8.0 g/cm³.

Three specimens were printed with the same parameters the only difference being the orientation of the parts in *xy*-axis of the powder bed. Specimen 1 was oriented with microfeatures being aligned with the *x*-axis, microfeatures of specimen 2 were parallel to *y*-axis and specimen 3 was tilted for 45° with respect to the specimen 1.

2.3. PeP setup and process parameters

A Pilot plant vat/immersion based PeP machine with a maximum output current of 150 A was used (Fig. 1a). A stainless-steel vat (max. volume of 200 l) was used as a cathode and a spring clamp was holding the specimen immersed in the electrolyte (Fig. 1b).



Fig. 1 (a) Pilot plant PeP machine, (b) Holder for the specimen

The previously obtained process parameters for used material to achieve high material removal rate, low surface roughness and high brightness were applied. The used electrolyte was a water solution of ammonium sulphate (0.33 M). The temperature of the electrolyte was kept at 80°C and the specimen was anodically polarized, to sustain the current density of about 0.2 A/cm², with the voltage of 350 V. The first specimen was treated for 10 min, the second for 15 min and the third for 20 min.

2.4. Microfluidic platform geometry

The design of microfeatures of the microfluidic platform is consistent with the feature shapes that are commonly applied in bottom grooved micromixers. The characteristic grooves at the bottom of the microchannel are either slanted at an angle of 45° with respect to the microchannel (so called slanted grooves - SG) or in a shape of a staggered herringbone (so called herringbone grooves – SH) (Fig. 2). The optimal aspect ratios of grooves (*d/a*) are a function of the microchannel aspect ratio (*h/w*) and were determined from research papers [9,10]. One should note, that the optimal aspect ratio of a SH groove is smaller compared to optimal SG groove.

Three sizes (L, M, S) of sample micromixer geometries were incorporated in the specimen design (Fig. 3). The

dimensions of geometries are gathered in Table 1. Depths of features were set so, that they correspond to a multiplier of a single layer powder depth of 40 μm .

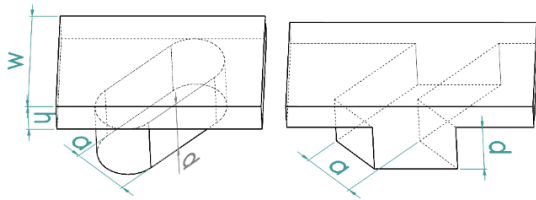


Fig. 2 The shape of a SG (left) and SH (right) grooves. Denotations of geometries are also presented

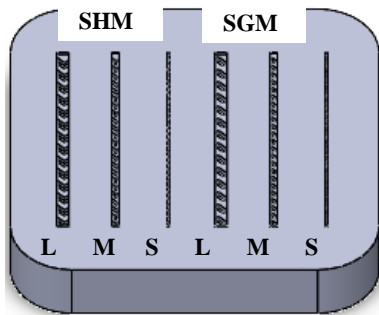


Fig. 3 3D model of a microfluidic specimen (30x30x3 mm) with denotations: SHM – staggered herringbone micromixer design, SGM – slanted groove micromixer design

Samples of groove micromixer geometries were modelled as parallel microchannels with descending sizes from large (L) to small (S).

Table 1 Nominal dimensions of micromixer designs

Variant	Microfeature			
	w [μm]	h [μm]	a [μm]	d [μm]
SGM-L	1000	280	500	480
SGM-M	600	160	300	320
SGM-S	200	80	100	80
SHM-L	1000	280	500	400
SHM-M	600	160	300	240
SHM-S	200	80	100	80

2.5. Measurements

Characterisation measurements were conducted on a Keyence VHX-6000 digital microscope. The 3D surface was acquired using depth composition function. Profile roughness (Ra) was determined by MarSurf PS 10 profilometer.

3. RESULTS AND DISCUSSION

3.1. SLM printed specimens

The first observation of printed microfluidic platforms is, that different orientation of the parts on the machine xy table did not result in different print quality. This is due to

the fact, that the laser trajectory at microfeature edges follows the edge contour, thus bulk hatch orientation influences only larger surfaces not crucial for microfeature geometries. Correspondingly, all the edges of microfeatures have a ridge of approximate height of $\sim 10 \mu\text{m}$.

As expected, larger (L) micromixer designs are printed with better geometrical quality (Fig. 4a,d). However, solidified microspheres with the diameter of used metal dust can be observed on the side walls of the microchannel and in the grooves (Fig. 5). Middle (M) sized designs are printed with bigger defects. In the grooves often a micropillar is present, which is a consequence of agglomerated resolidified dust particles (Fig. 6(left)). The explanation of mentioned artefacts lies in presence of dust particles near the edges of microfeatures which should not be melted by laser beam, however, they are melted due to excess heat. For the smallest designs (S) the microgrooves are below the printer's resolution (e.g. diameter of laser focus point is $100 \mu\text{m}$) thus, they are printed into shapes that hardly correspond to a groove (Fig. 4c,f). Corresponding microchannels are printed more reliably with high relative width deviation.

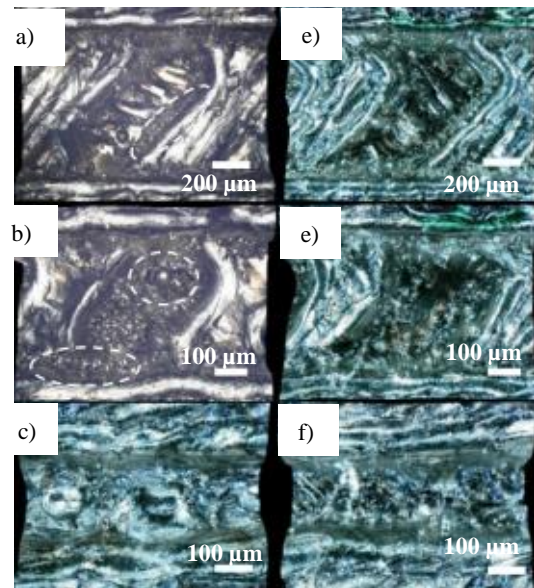


Fig. 4 Microscope images of single grooves (specimen 1). (a) SG-L, dashed ellipse highlights solidified spheres, (b) SG-M, in the groove a micropillar and solidified spheres at the channel edge are highlighted, (c) SG-S, (d) SH-L, (e) SH-M and (f) SH-S.

The surface roughness was measured in the middle part of the specimens. The Ra value for all three specimens was measured to be $18.5 \pm 0.4 \mu\text{m}$, which is in a typical range for SLM printed parts. This roughness exceeds the values for typical microfluidic applications ($Ra < 1 \mu\text{m}$) by a lot, thus specimens were subjected to PeP treatment to reduce it.

3.2. Specimens after PeP treatment

At larger micromixer designs even after the shortest PeP treatment (specimen 1) significant improvement of the microfeatures quality is observed. Formed microspheres at

the edges and on the bottom of the grooves were removed (Fig. 5). This is because higher electric field is present at pointy artefacts thus the PeP process removes them. Also, the waviness due to the laser scanning hatch pattern got severely reduced. Similar observations can be made with regards to medium sized microfeatures. Furthermore, the occasional micropillars within the grooves were also removed by the PeP as is evident from Fig. 6. However, a damaging effect of PeP can be observed on groove edges where excessive material removal occurred.



Fig. 5. Pre (left) and post (right) PeP treated specimen 1 detail (SG-L). The arrows point to solidified microspheres at the side and bottom of the groove.

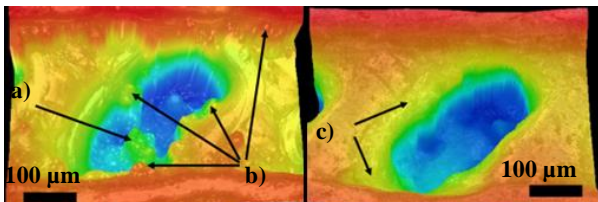


Fig. 6. A colored height microscopic image of a SG-M groove before (left) PeP treatment. Arrows (a) point at a micropillar and (b) at microspheres at the microfeature edges. SG-M groove after PeP treatment (right). Arrows (c) point at excessive erosion at groove edge

The influence of the PeP treatment duration can be extrapolated from Fig. 7. After shortest treatment time (10 min, Fig. 7b) the effects are consistent with above observations, namely, the microspheres and possible micropillars were eroded.

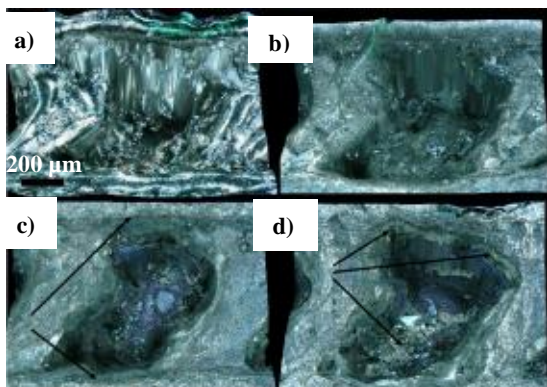


Fig. 7. SH-M grooves after PeP treatment. (a) Untreated groove (specimen 1), (b) PeP treated for 10 min (specimen 1), (c) 15 min (specimen 2) where arrows point at microchannel wall material removal and (d) 20 min (specimen 3), where arrows point to microcracks at the edge and the bottom of the groove.

Longer PeP treatment (15 min, Fig. 7c) resulted in significant material removal also at the main channel side walls. 20 min PeP treatment (Fig. 7d) resulted in greater

deterioration at the microchannel side walls. Furthermore, microcracks appeared at the groove edges and bottom.

The roughness on the flat surfaces of specimens was significantly reduced. Similar Ra values were measured on all three specimens regardless of the PeP treatment duration. For specimen 1 average roughness value was $2.7 \pm 0.3 \mu\text{m}$, for specimen 2 $2.8 \pm 0.3 \mu\text{m}$ and specimen 3 $2.5 \pm 0.3 \mu\text{m}$. This means that the shortest PeP treatment was the best option since low frequency waviness of the pre-treated parts is harder to remove. However, the roughness still exceeds the values acceptable in microfluidics.

6. CONCLUSIONS

In this paper, the influence of PeP treatment of SLM printed microfluidic platforms is presented. The results show that PeP treatment significantly improves microfeatures quality by removing resolidified microspheres at the feature edges and reduces overall roughness. Even the occasional occurrence of micropillar artefacts in the medium sized grooves were removed. Three durations of PeP were tested and the shortest treatment has proved to be the best. At longer PeP times, the edges of the microfeatures got eroded and there is a possibility of material surface microcracking.

This brief investigation shows, that PeP is a promising post-treatment technology which can improve the SLM printed microfluidic platforms quality.

ACKNOWLEDGEMENTS

This work was supported by the Slovenian Research Agency (ARRS) (Grant No. P2-0248 (B)) and EU EC H2020 funded Era Chair of Micro Process Engineering and Technology – COMPETE (Grant No. 811040). Authors wish to thank Boštjan Podlipec and SiEVA ltd. for providing resources for SLM printing.

REFERENCES

- [1] Waheed, S., Cabot, J. M., Macdonald, N. P., Lewis, T., Guijt, R. M., Paull, B., and Breadmore, M. C., 2016, *3D Printed Microfluidic Devices: Enablers and Barriers*, *Lab Chip*, 16(11), pp. 1993–2013.
- [2] Guo, N., and Leu, M. C., 2013, *Additive Manufacturing: Technology, Applications and Research Needs*, *Front. Mech. Eng.*, 8(3), pp. 215–243.
- [3] Alting, L., Kimura, F., Hansen, H. N., and Bissacco, G., 2003, *Micro Engineering*, *CIRP Ann. - Manuf. Technol.*, 52(2), pp. 635–657.
- [4] Gjuraj, E., Kongoli, R., and Shore, G., 2012, *Combination of Flow Reactors with Microwave-Assisted Synthesis: Smart Engineering Concept for Steering Synthetic Chemistry on the 'Fast Lane.'* *Chem. Biochem. Eng. Q.*, 26(3), pp. 285–307.

- [5] Nagarajan, B., Hu, Z., Song, X., Zhai, W., and Wei, J., 2019, *Development of Micro Selective Laser Melting: The State of the Art and Future Perspectives*, *Engineering*, 5(4), pp. 702–720.
- [6] Zeidler, H., Böttger-Hiller, F., Krinke, S., Parenti, P., and Annoni, M., 2019, *Surface Finish of Additively Manufactured Parts Using Plasma Electrolytic Polishing*, 19th International Conference and Exhibition, EUSPEN 2019, pp. 228–229.
- [7] Zeidler, H., and Böttger-Hiller, F., 2018, *Surface Finish of Additively Manufactured Parts Using Plasma Electrolytic Polishing*, WCMNM 2018, J. Valentinčič, M.B.-G. Jun, K. Dohda, and S.S. Dimov, eds., Research Publishing, Singapore, Portorose, Slovenia.
- [8] Parfenov, E. V., Yerokhin, A., Nevyantseva, R. R., Gorbakov, M. V., Liang, C. J., and Matthews, A., 2015, *Towards Smart Electrolytic Plasma Technologies: An Overview of Methodological Approaches to Process Modelling*, *Surf. Coatings Technol.*, 269(1), pp. 2–22.
- [9] Sabotin, I., Tristo, G., Junkar, M., and Valentinčič, J., 2013, *Two-Step Design Protocol for Patterned Groove Micromixers*, *Chem. Eng. Res. Des.*, 91(5).
- [10] Lynn, N. S., and Dandy, D. S., 2007, *Geometrical Optimization of Helical Flow in Grooved Micromixers*, *Lab Chip*, 7(5), pp. 580–587.

NOTE

This paper is based on the paper presented at 14th International scientific conference MMA 2021 - FLEXIBLE TECHNOLOGIES Novi Sad, Serbia, September 23-25, 2021.